ELSEVIER

15 July 1996

OPTICS COMMUNICATIONS

Optics Communications 128 (1996) 281–286

Pattern formation in a linear photorefractive oscillator

A.V. Mamaev [1], M. Saffman

Department of Optics and Fluid Dynamics, Risø National Laboratory, DK-4000 Roskilde, Denmark

Received 1 November 1995; accepted 27 February 1996

Abstract

We report on spatial patterns in a linear photorefractive oscillator pumped by counterpropagating beams. Both spatially periodic and irregular patterns are observed depending on the cavity to pump laser detuning and the relative intensity of the two pump beams.

Several different mechanisms lead to pattern formation in nonlinear optics. A very general mechanism is the transverse modulational instability of counterpropagating beams [1–3]. The nonlinear stage of this instability leads to regular transverse patterns, often with hexagonal symmetry [3,4]. This type of instability occurs when two beams counterpropagate in a passive nonlinear medium, without any feedback from cavity mirrors. The instability has been observed in a wide variety of materials, including atomic vapors [4], liquid crystals [5], photorefractives [6] and organic films [7].

The situation in active nonlinear media that are placed in an optical cavity, and pumped by an external source of energy, is more complicated. A distinction should be made between the case of an optical cavity that supports a spectrum of stable linear modes, and the opposite situation where the optical cavity is unstable, or only marginally stable. Pattern formation in cavities with a finite spectrum of stable linear modes may be understood in terms of the nonlinear excitation of a superposition of these linear modes [8,9]. The resulting patterns may be static or dynamic depending on whether or not the modes are frequency degenerate [10,11]. Patterns that are superpositions of linear cavity modes have the property that they are similar to their own Fourier transform. Thus, near and far-field pictures look the same up to a scaling factor.

On the other hand a cavity formed by plane parallel mirrors has only marginally stable modes. These modes take the form of cylindrically symmetric rings that correspond to Fabry-Perot resonances. The angle between the rings and the optical axis depends on the cavity tuning. We show below that in the presence of counterpropagating pump beams these rings become unstable and collapse into tilted waves lying on the rings, but propagating at an arbitrary azimuthal angle. Excitation of tilted waves has been shown numerically to lead to a rich variety of patterns in both linear [12] and ring geometries [13]. We present the first, to our knowledge, experimental observation of this mechanism, using a linear geometry with a photorefractive crystal as the active gain medium. There are two instability thresholds in this system. The first is the laser threshold at which oscillation commences and takes the form of Fabry-Perot rings in the far field. This is most easily observable with a single external

[1] Permanent address: Institute for Problems in Mechanics, Russian Academy of Sciences, Vernadskogo 101, Moscow 117526, Russia.

PII S0030-4018(96)00158-7

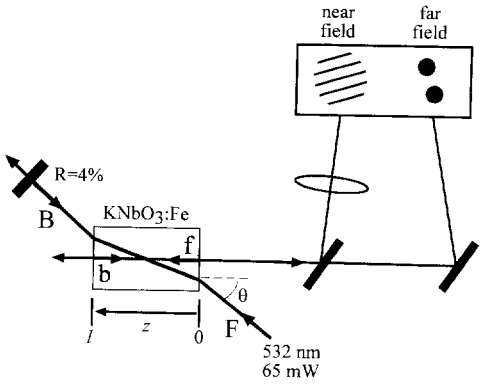

Fig. 1. Experimental setup. The laser power is 65 mW focused to a spot of Gaussian diameter 0.85 mm. The crystal length is $l = 5.2$ mm, and $\theta = 9.7°$.

pump beam. At the second threshold, which is passed when a second pump beam is introduced, the rings become unstable, and collapse to a finite number of tilted waves. These patterns are not Fourier self-similar and the near and far field intensity distributions are not related by a simple rescaling of coordinates. In this sense these patterns are similar to those observed in cavityless systems, and qualitatively different from those observed in cavities containing focusing elements and well-defined stable modes.

The experimental geometry is shown in Fig. 1. A crystal of $KNbO_3$ doped with 0.5% by weight Fe is illuminated by counterpropagating beams. The forward pump beam F is derived from a Nd:YAG laser at 532 nm. The counterpropagating pump B is formed by reflection from a mirror of intensity reflectivity of 4% located about 15 mm from the crystal. A Faraday rotator is used to isolate the laser from beam B. Scattered light seeds the oscillation of beams f and b between the uncoated c-faces of the crystal, each having a reflectivity of about 15%. In this geometry, with propagation almost parallel to the crystal c-axis, reflection gratings form and couple beam pairs $\{F,B\}$, $\{F,b\}$, $\{f,B\}$, and $\{f,b\}$. In $KNbO_3$ the gratings are shifted by $\pi/2$ with respect to the optical interference pattern, so that there is strong coupling of energy from the beams propagating along $-\hat{c}$ to those propagating along $+\hat{c}$.

When a mirror with high reflectivity is placed after the crystal we observe the normal transverse modulational instability of F and B leading to hexagonal patterns [6]. When the mirror is removed so there is no beam B excitation of the Fabry-Perot resonances of the linear cavity is observed, as shown in Fig. 2. When the crystal length is such that the on-axis mode is off resonance we observe the patterns shown in Fig. 2a. Since absorption of light in the crystal contributes to the thermal loading, and hence to the index of refraction of the crystal, it is possible to tune the resonance condition to a certain degree by varying the laser power. When the power is adjusted to bring the on-axis mode on resonance we observe the patterns shown in Fig. 2b. The near field pictures in this, and subsequent figures, are magnified images of the field at the $z = 0$ end of the crystal. The near-field is characterized by dark structures (field dislocations and stripes) that drift across the aperture. The drift motion is due to the crystal end faces not being exactly parallel. Even though there is only one external pump beam, the second pump beam B is present to the extent that it is generated by the four-wave mixing geometry [14]. For the conditions of Fig. 2. we observe a beam, much weaker than the oscillating beams, counterpropagating to F.

When the 4% reflectivity mirror is inserted the patterns change dramatically as shown in Fig. 3. The Fabry-Perot rings that are observed with a single pump beam become unstable and collapse to two or more tilted waves in the far-field, leading to regular roll, tiled, and rhombic patterns in the near field. Simultaneous excitation of multiple tilted waves gives rise to coexisting near-field patterns of different symmetries. In some cases waves corresponding to several different Fabry-Perot rings are excited simultaneously. The orientation of the roll patterns shown in Fig. 3a was arbitrary for well aligned pump beams. Adjusting the feedback mirror to give a small misalignment between F and B resulted in rolls with fringes parallel to the transverse vector $\delta k = k_F + k_B$. Note that the far-field patterns all have inversion symmetry. This is a consequence of the bidirectional pumping geometry. The patterns change qualitatively with a characteristic time of about one minute. We believe these slow drifts are due to thermal changes in the effective length, and hence the resonance condition of the crystal.

A qualitative change in the near-field patterns is observed when the laser power is adjusted so that the on-axis mode is in resonance. Examples of these patterns are shown in Fig. 4. In this case a variety of irregular structures are seen. These include finger-like contours, zig-zag boundaries, rolls, and coexisting combinations

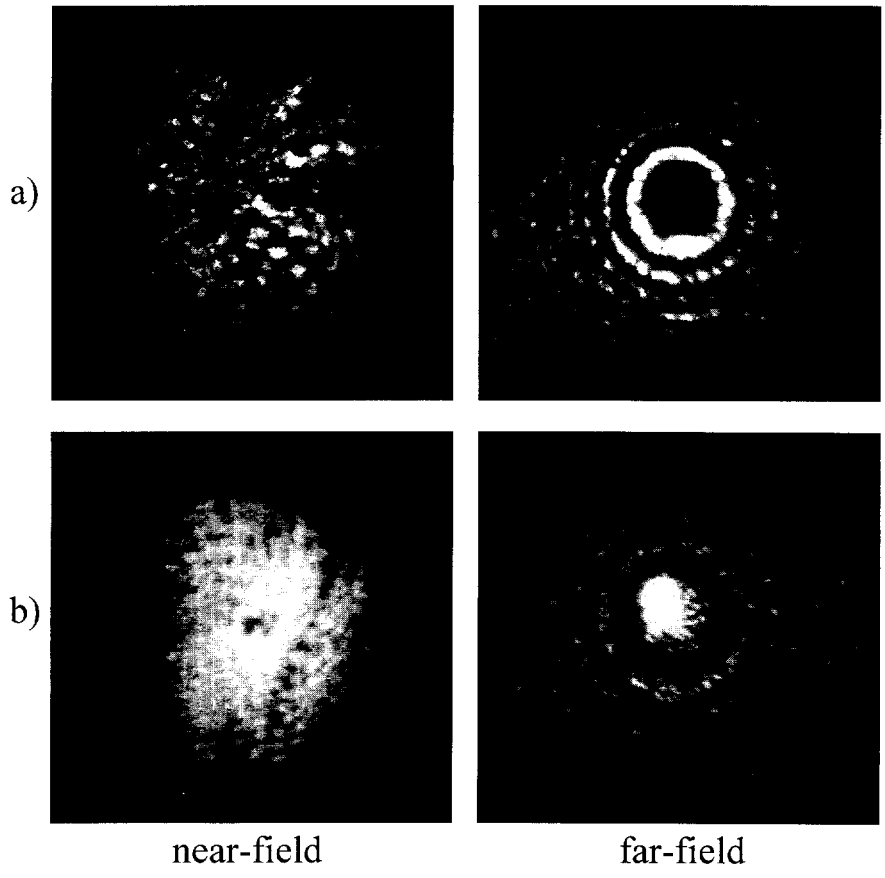

Fig. 2. Characteristic near and far field oscillation patterns with a single pump beam.

of these structures. Patterns with a large degree of spatial complexity are observable since the cavity Fresnel number given by $F = w_{\text{pump}}^2/(\lambda l)$ is about 160, which is much greater than unity. The patterns are dynamic and evolve continually with a characteristic time scale of seconds. This time scale is much longer than the characteristic photorefractive time constant which, for the given pump beam intensity, is of the order of 0.05 s, yet much shorter than the time scale associated with thermal drifts.

When the cavity is in resonance with the pump radiation the generated beams have strong components lying along the cavity axis. In general these beams have a finite angular divergence, and they contain components that are frequency shifted with respect to the pumps, so that they experience both energy and phase coupling. This leads to the nonstationary, irregular patterns shown in Fig. 4. When the cavity is not in resonance with the pump radiation tilted waves satisfying $\theta_c + (k_\perp^2/2k)l = 0$, where θ_c is the cavity detuning and $k_\perp$ is the transverse wavevector, will be resonant with the pump. In this case there is a well defined spatial scale given by $\Lambda \sim \sqrt{l/(2k\theta_c)}$ [13], and we observe mostly periodic patterns as shown in Fig. 3.

As described above three different modes of operation, namely Fabry-Perot rings (Fig. 2), transverse modulational instability of the pumps, and tilted wave patterns (Figs. 3, 4), are all possible depending on the relative intensity of the pump beams. The coupling coefficient for reflection gratings in the heavily doped $KNbO_3$ used here was $|\gamma l| \sim 6$, so the strong longitudinal coupling must be accounted for. We will calculate the oscillation threshold condition using the reflection grating equations of motion [14,15]:

$$\frac{\partial F}{\partial z'} - \frac{i}{2k}\nabla_{r'_\perp}^2 F = GB + gb, \tag{1}$$

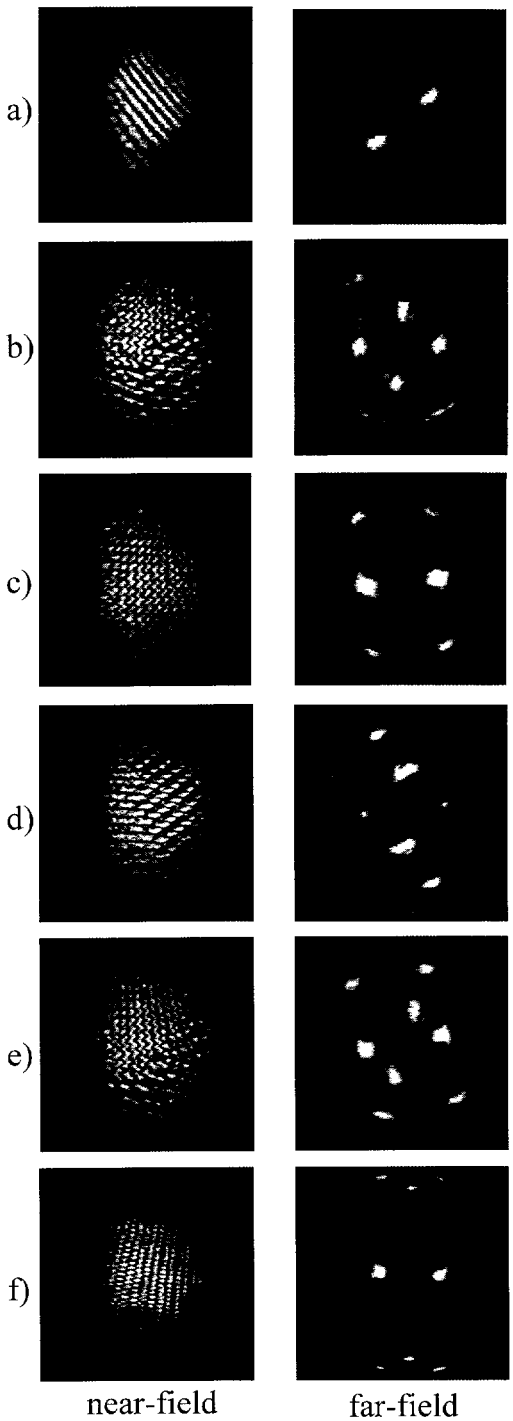

Fig. 3. Periodic patterns: (a) rolls, (b) mixed symmetry, (c) tiles, (d) coexisting rolls and rhomboids, (e) wavy stripes, and (f) crossed rolls. Left column near-field, right column far-field.

$$\frac{\partial B}{\partial z'} + \frac{i}{2k}\nabla^2_{r'_\perp} B = G^* F + g^* f, \tag{2}$$

$$\frac{\partial f}{\partial z} - \frac{i}{2k}\nabla^2_{r_\perp} f = gB, \tag{3}$$

$$\frac{\partial b}{\partial z} + \frac{i}{2k}\nabla^2_{r_\perp} b = g^* F, \tag{4}$$

$$\left(\tau\frac{\partial}{\partial t} + 1\right) G = i\frac{\gamma}{I} FB^*, \tag{5}$$

$$\left(\tau\frac{\partial}{\partial t} + 1\right) g = i\frac{\gamma}{I}\left(Fb^* + fB^*\right). \tag{6}$$

Coupling due to transmission gratings has been ignored, since both the effective electro-optic coefficient for this type of grating, and the angle between the co-propagating beams, are small. Here γ is the photorefractive coupling constant, $I = |F|^2 + |B|^2 + |f|^2 + |b|^2$ is the intensity, and τ is the material relaxation time. The pump beams propagate along coordinate z' and coordinate r' lies in the plane perpendicular to z'. The grating G that is responsible for direct interaction of the counterpropagating pumps is typically neglected in standard treatments of reflection grating four-wave mixing [14,15]. In the present case the pump beams F and B are mutually coherent, and have the same polarization, so this grating cannot be ignored. An additional grating proportional to the product fb^* has been neglected since the generated beams f and b will be assumed small in the following threshold analysis. Reflection gratings in $KNbO_3$ are due almost exclusively to a diffusive charge transport mechanism so that the index grating is shifted by $\pi/2$ with respect to the optical interference pattern. The coupling constant γ is thus purely imaginary.

When the feedback mirror has unity reflectivity $F(l) = B(l)$, and the threshold for transverse modulational instability of beams F and B is $|\gamma l| \simeq 6$ [16]. Since the oscillation threshold for beams f and b is much lower than this at small B it can be found by describing F and B as plane waves and linearizing in the amplitudes f, b. We assume the cavity to be in resonance with the pump radiation. If this were not the case the oscillation would be off-axis, but this does not change the results of the threshold analysis. The resulting steady state plane wave equations then take the form

$$\frac{\partial F}{\partial z} = -\gamma'' \frac{q}{1+q} F, \tag{7}$$

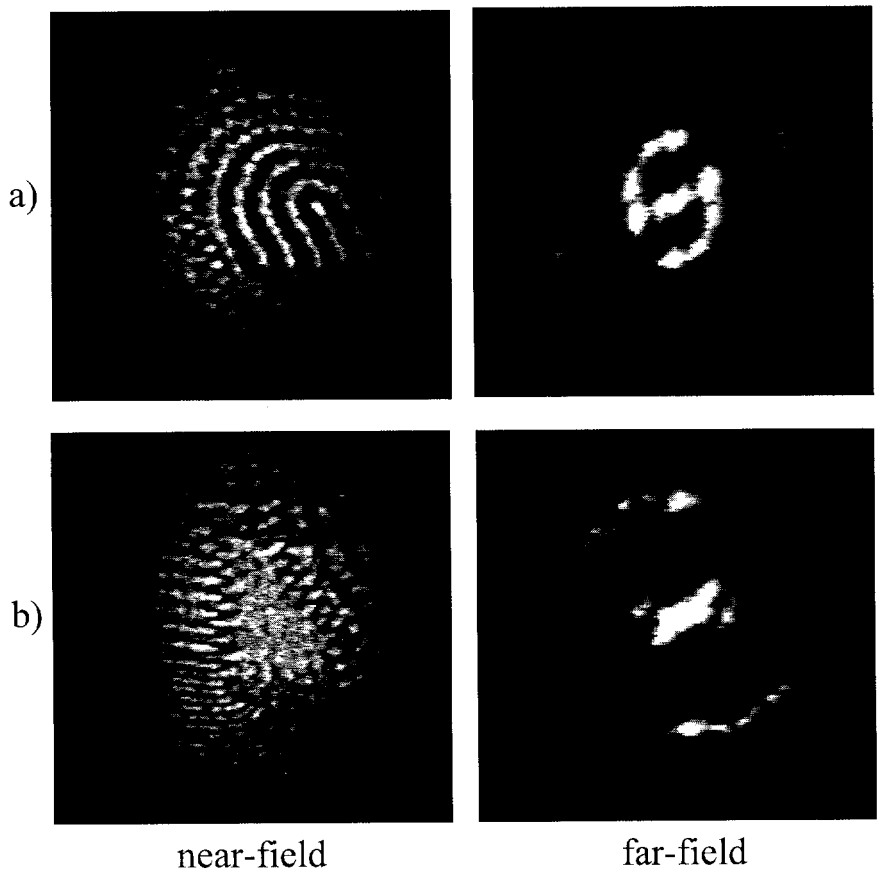

Fig. 4. Complex patterns: (a) finger pattern, (b) coexisting uniform, zig-zag and roll regions. Left column near-field, right column far-field.

$$\frac{\partial B}{\partial z} = -\gamma'' \frac{1}{1+q} B, \tag{8}$$

$$\frac{\partial \tilde{f}}{\partial z} = -\gamma'' \frac{q}{1+q} \tilde{b}^*, \tag{9}$$

$$\frac{\partial \tilde{b}^*}{\partial z} = -\gamma'' \frac{1}{1+q} \tilde{f}, \tag{10}$$

where $\gamma = i\gamma''$, $\tilde{f} = f/F$, $\tilde{b} = b/B$, $q(z) = |B(z)|^2/|F(z)|^2$, and we have replaced z' by z in the first two equations above since $\cos(\theta) \approx 1$.

For no feedback mirror we have unidirectional pumping with $B = 0$ and $q = 0$. Hence f propagates as in free space, and b and f only couple weakly due to pump depletion. It is thus not surprising that for modest nonlinearity, where the depletion of F by f as given by Eq. (1) is small, unidirectional pumping leads to excitation of the normal Fabry-Perot resonances as seen in the far-field views shown in Fig. 2.

Eqs. (7)–(10) yield immediately the threshold condition $\gamma'' l = -\ln R_c \sim 1.9$ where $R_c = 0.15$ is the reflectivity of the crystal faces.

For a perfectly reflecting feedback mirror ($F(l) = B(l)$) we have $q(z) = 1$ and the oscillation threshold is infinite since the amplification of b by pump F is counterbalanced by the depletion of f due to pump B. For general values of F and B $q = q(z)$ and Eqs. (9), (10) have space dependent coefficients. To proceed we approximate the factors $q/(1+q)$ and $1/(1+q)$ in Eqs. (9), (10) by their longitudinal averages $q_1 = (1/l)\int_0^l \mathrm{d}z\, q/(1+q)$ and $q_2 = (1/l)\int_0^l \mathrm{d}z\, 1/(1+q)$. The oscillation condition is then determined by the expression

$$\tanh(\sqrt{q_1 q_2}\,\gamma'' l) = \left(\frac{m q_2}{R_c t_F q_1}\right)^{1/2} \frac{1 - R_c t_F \mathrm{e}^{\gamma'' l}}{1 - m(q_2/q_1)\,\mathrm{e}^{\gamma'' l}}. \tag{11}$$

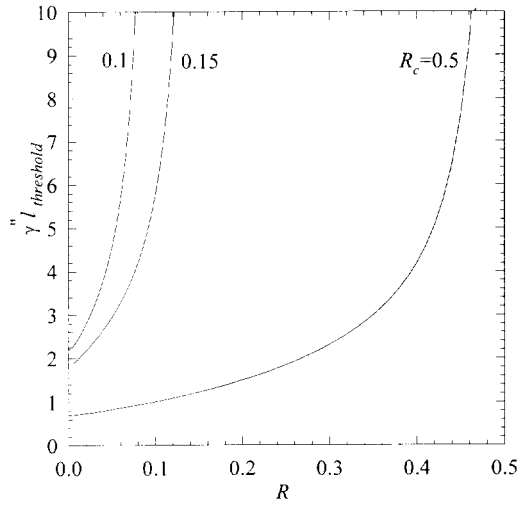

Fig. 5. Oscillation threshold as a function of feedback mirror reflectivity for $R_c = 0.1, 0.15$, and 0.5.

Here $m = B(l)^2/F(0)^2 = Rt_F$, $t_F = (1+m)/(1+me^{2\gamma'' l})$ [17], and R is the feedback mirror reflectivity. The dependence of the threshold coupling on R is shown in Fig. 5. For small R linear oscillation is preferred, while for large R modulational instability of the pumps has a lower threshold. As R_c is reduced oscillation is restricted to smaller values of R. This calculation gives the threshold for oscillation of beams f and b in ring modes. Calculation of the second threshold, at which the rings collapse to tilted waves, will be considered in future work. It is noteworthy that the change in the oscillation structure, that is observed in the presence of beam B, is accompanied by a reduction in the oscillating power, since B depletes beam f.

In summary we have observed periodic and irregular patterns in a linear photorefractive oscillator. Periodic patterns arise from a tilted wave mechanism. The observed patterns depend strongly on the relative intensities of the counterpropagating pump beams.

Acknowledgements

This work was supported by a grant from the Danish Natural Science Research Council.

References

[1] S.N. Vlasov and V.I. Talanov, in: Optical Phase Conjugation in Nonlinear Media, ed. V.I. Bespalov (Institute of Applied Physics, USSR Academy of Sciences, Gorki, 1979).
[2] W.J. Firth and C. Paré, Optics Lett. 13 (1988) 1096.
[3] G. Grynberg, Optics Comm. 66 (1988) 321.
[4] G. Grynberg, E. Le Bihan, P. Verkerk, P. Simoneau, J.R.R. Leite, D. Bloch, S. Le Boiteux and M. Ducloy, Optics Comm. 67 (1988) 363.
[5] R. Macdonald and H.J. Eichler, Optics Comm. 89 (1992) 289.
[6] T. Honda, Optics Lett. 18 (1993) 598.
[7] J. Glückstad and M. Saffman, Optics Lett. 20 (1995) 551.
[8] L.A. Lugiato, C. Oldano and L.M. Narducci, J. Opt. Soc. Am. B 5 (1988) 879.
[9] C. Green, G.B. Mindlin, E.J. D'Angelo, H.G. Solari and J.R. Tredicce, Phys. Rev. Lett. 65 (1990) 3124.
[10] M. Brambilla, M. Cattaneo, L.A. Lugiato, R. Pirovano, F. Prati, A.J. Kent, G.-L. Oppo, A.B. Coates, C.O. Weiss, C. Green, E.J. D'Angelo and J.R. Tredicce, Phys. Rev. A 49 (1994) 1427.
[11] A.B. Coates, C.O. Weiss, C. Green, E.J. D'Angelo and J.R. Tredicce, M. Brambilla, M. Cattaneo, L.A. Lugiato, R. Pirovano, F. Prati, A.J. Kent and G.-L. Oppo, Phys. Rev. A 49 (1994) 1452.
[12] P.K. Jakobsen, J. Lega, Q. Feng, M. Staley, J.V. Moloney and A.C. Newell, Phys. Rev. A 49 (1994) 4189.
[13] W.J. Firth and A.J. Scroggie, Europhys. Lett. 26 (1994) 521.
[14] M. Cronin-Golomb, B. Fischer, J.O. White and A. Yariv, IEEE J. Quantum Electron. QE-20 (1984) 12.
[15] V.T. Tikhonchuk and A.A. Zozulya, Prog. Quantum Electron. 15 (1991) 231.
[16] M. Saffman, A.A. Zozulya and D.Z. Anderson, J. Opt. Soc. Am. B 11 (1994) 1409.
[17] P. Yeh, Optics Comm. 45 (1983) 323.